Guidelines for application of computer-assisted indocyanine green molecular fluorescence imaging in diagnosis and surgical navigation of liver tumors (2019)

Digital Medical Association of Chinese Medical Association; Digital Intelligent Surgery Professional Committee of Chinese Research Hospital Association; Liver Cancer Professional Committee of Chinese Medical Doctor Association; Clinical Precise Medicine Professional Committee of Chinese Medical Doctor Association; Medical Imaging and Equipment Professional Committee of China Graphics Society; Molecular Imaging Professional Committee of China Biophysical Society

Abstract: Computer-assisted combined indocyanine green (ICG) molecular fluorescence imaging technology can be used for preoperative planning and intraoperative detection from three-dimensional (3D) morphological anatomy and level of cellular function to guide the anatomical, functional and radical hepatectomy of liver tumor. This technology has received wide acceptance and has shown important diagnostic and therapeutic value. This guideline is intended to standardize the application of computer-assisted combined ICG molecular fluorescence imaging for accurate diagnosis and treatment of liver tumors in the following aspects: (1) the workflow of 3D visualization technology; (2) the mechanism and application flow of ICG molecular fluorescence imaging; (3) clinical application of 3D visualization technology and virtual reality technology; and (4) clinical application of ICG molecular fluorescence imaging. ICG molecular fluorescence imaging can help to define tumor boundary, determine hepatic segment and hepatic lobectomy tangent at the molecular and cellular level, and detect small lesions or metastases. According to the fluorescence signal characteristics of liver tumors and combined with rapid frozen pathological examination during operation, the differentiation degree of liver space-occupying lesions (such as primary liver cancer) can be preliminarily determined, and residual tumors and biliary leakage on the hepatic section can be detected after hepatectomy. Computer-assisted ICG molecular fluorescence imaging in the diagnosis and surgical navigation of liver tumors provides a new approach to digital diagnosis and treatment of liver tumors. With its development in clinical practice and the technological innovation, this technology will be further improved to allow more accurate diagnosis and treatment of liver tumors.

Keywords: indocyanine green; fluorescence imaging; three-dimensional visualization technology; liver tumor; surgical navigation

1. INTRODUCTION

Three-dimensional visualization technology (3DVT) is used to display, describe, and explain the 3D anatomical and morphological features of tissues and organs, and has been widely used in liver surgery. The protein-binding

indocyanine green (ICG) is a near-infrared fluorescent dye and can be activated by extraneous light with a wavelength of 750-810 nm to emit 840 nm near-infrared light [1]. Since the first description of its use to guide hepatectomy in 2009 [2], ICG molecular fluorescence imaging technique has been widely used as an auxiliary tool at the cell function level for the diagnosis and surgical navigation of liver tumors [3-6].

ICG molecular fluorescence imaging technology is capable of defining the tumor boundary, the hepatic segments and the left and right hepatectomy line at both molecular and cellular levels, and allows detection of small lesions or metastases and intraoperative scanning of the liver using fluorescence detection equipment. The fluorescence signal characteristics of liver tumors combined with intraoperative rapid frozen pathological examination help to preliminarily determine the differentiation of space-occupying lesions in the liver (such as primary liver cancer) and detect residual tumors and biliary leakage after hepatectomy. Computer-assisted ICG molecular fluorescence imaging can guide the preoperative planning and intraoperative detection of

liver tumors from the perspective of 3D morphological anatomy and cell function of the liver tissues, and has been proved for clinical application for its unique value in accurate diagnosis and treatment [7]. In 2017, expert consensus on the application of computer-assisted ICG molecular fluorescence imaging in the diagnosis and surgical navigation of liver tumors was published in China. After nearly 3 years of clinical practice, this technology has now been widely used in China, and clinical studies have been carried out with encouraging results [8]. In view of this, the experts from Digital Medical Association of Chinese Medical Association, Digital Intelligent Surgery Professional Committee of Chinese Research Hospital Association and Liver Cancer Professional Committee of Chinese Medical Doctor Association developed the 2019 edition of the guideline for the application of computer-assisted ICG molecular fluorescence imaging technology in the diagnosis and surgical navigation of liver tumor based on the consensus of the 2017 Edition. The aim of this guideline is to provide guidance and reference for surgeons engaging in, or aspiring to engage in the diagnosis and treatment model.

The guideline refers to the Grading of Recommendations Assessment, Development and Evaluation (GRADE), which divides the quality of evidence into high, moderate, and low/very low levels [8-10]. The levels of evidence are reported using the letter grades of A, B and C, respectively. The guideline is developed with the participation of experts from relevant fields and two patient representatives in China. The experts and patient representatives who participated in the formation of recommendation opinions signed a declaration of no conflict of interest in advance, which was checked by the secretariats of the societies for the development of the guideline. The strength of the recommendations was classified into strong and weak recommendations.

2. Application of three-dimensional visualization technology

2.1 Data acquisition and storage quality control

Setting of computed tomography (CT) scanning parameters and data storage (taking 64-slice CT as the example): the patient takes a supine position in a head-foot direction, and is scanned from the top of the diaphragm to the lower edge of the kidney. The scanning parameters: 120 kV, 250 mA; a 0.625×64 row detector combination; layer thickness 1.0 mm, pitch 0.984, and per rotation time of the spherical tube 0.5 s. The delay time is 20-25 s for arterial phase scan and 50-55 s for portal vein phase. After the scanning, the image data are transferred to the post-processing workstation of CT, and the three-stage data (plain scan, arterial phase and portal vein phase) are stored [11-13].

2.2 Establishment and homogenization of quality control system for 3D reconstruction

3D reconstruction should follow the following quality control and homogenization criteria: (1) The patients is instructed to hold their breath during CT scanning to avoid potential difficulties in subsequent image segmentation and registration; (2) The quality of original CT images meets the minimum standard of 3D reconstruction software; (3) 3D reconstruction is performed by qualified personnel; (4) 3D models are manually checked and modified by senior surgeons and radiologists. Only after standardization and strict quality control can the 3D visualization models be used to guide clinical practice. CT image data are imported into 3D visualization imaging system to segment, register and reconstruct abdominal organs, abdominal vascular system and liver tumors. Individualized liver segmentation, liver volume calculation and virtual hepatectomy are carried out according to the need. The 16 key points in quality control and scoring of 3D visualization diagnosis and treatment are described in Tab.1.

Recommendation: Surgeons should cooperate with radiologists to setup standardized scanning parameters to obtain high-quality CT image data. Based on this, 3D visualization studies should be carried out according to the available equipment, conditions, and clinical needs (Strong recommendation).

3. Mechanism and application of ICG molecular fluorescence imaging

3.1 Mechanism of targeted retention of ICG in liver tumors

The uptake of ICG is mediated mainly by the organic anion transporting polypeptide 1B3 (OATP1B3) and Na$^+$-taurocholate cotransporting polypeptide (NTCP) in hepatic cells, and ICG is excreted mainly via the multidrug resistance-associated protein 2 (MRP2) carrier system expressed on the bile capillary. After excretion, ICG does not participate in the enterohepatic circulation [14-15]. Therefore, in normal hepatic tissues, ICG can rapidly enter hepatic cells and emits fluorescence under an exciting light. The fluorescence gradually fades after ICG excretion through the biliary system. In hepatic tumors or cirrhotic nodules where the biliary excretory function of hepatic cells is impaired, targeted ICG retention occurs to cause delayed fluorescence fading.

3.2 Preparation and administration of ICG

The sulfate group in the polycyclic structure of ICG determines that sterile water for injection is the preferred solvent for ICG, but the aqueous solution of ICG is not stable and must be used within 6-10 h after dilution [16]. Saline must not be used when preparing ICG as it causes the aggregation of ICG molecules [1, 17]. The timing, patterns, and dosage of ICG injection can vary for different purposes and across different centers [18-21].

For optimal intraoperative fluorescence imaging of liver tumors, the timing of preoperative administration of ICG needs to be adjusted according to the ICG retention rate within 15 min (ICG R15) of the individual patients.

Tab.1 Process measures of 3D visualization

	Criteria	Points
1	Diagnosis of liver diseases by preoperative imaging (ultrasound, CT or MRI)	+1
2	Patients fast for at least 4 h prior to CT scan, orally take 0.5-1.0 L of clear liquid 20 to 30 min prior to the examination and take another 500 mL prior to the exam.	+1
3	Train the patient to hold their breath in full inspiration before scanning and instruct them to do so during each scan phase to achieve maximum management of artifacts due to respiratory motion.	+1
4	Select 64-slice or above spiral CT scanning with slice thickness of 0.625-1.0 mm.	+1
5	CT scanning ranges from the top of the diaphragm to the lower level of both kidneys, and furthermore perform dynamic abdominal scan after intravenous contrast medium administration; perform CT celiac arteriography. The arterial phase, portal venous phase and delayed phase scans start at a delay of 20-25 s, 50-55 s, and 2 min, respectively.	+1
6	3D reconstruction should be performed by attending physicians or a level above who are engaged in the diagnosis and treatment of liver diseases.	+1
7	Evaluate the integrity of the course, shape and continuity of hepatic artery reconstructed by 3D visualization to determine whether manual revision is required (manual revision is unnecessary when the tertiary branches of artery can be reconstructed).	+1 (no manual revision); -1 (manual revision required)
8	Evaluate the integrity of the course, morphology and continuity of hepatic vein reconstructed by 3D visualization to determine whether manual revision is required (manual revision is unnecessary if the tertiary branches of hepatic vein can be reconstructed).	+1 (no manual revision); -1 (manual revision) required
9	Evaluate the integrity of the course, morphology and continuity of portal vein reconstructed by 3D visualization to determine whether manual revision is required. The branches of the portal vein system with the diameter ⩾5mm should be reconstructed (which is unnecessary if the tertiary branches of portal vein can be reconstructed).	+1 (no manual revision); -1 (manual revision required),
10	Evaluate the course, morphology, continuity and integrity of the 3D reconstructed biliary tract (manual revision is unnecessary if the tertiary branches of biliary tree can be reconstructed).	+1 (biliary system reconstructed); -1 (no biliary system reconstructed)
11	Evaluate the morphology, size and distribution of lesions in the 3D reconstructed model and whether they are consistent with CT images.	+3 (basically consistent, no manual revision required): +2 (mostly consistent, manual revision required): -1 (inconsistent, manual revision required)
12	The overall 3D model should be validated by at least 2 abdominal imaging attendings and at least 2 attending hepatologists in comparison with the original CT images, and finally confirmed by a senior physician.	+1
13	Perform simulation surgery based on 3D model. The simulation of various schemes should be carried out and the optimal surgical approach and surgical resection plane should be selected by two attending physicians, and finally confirmed by a senior physician.	+2
14	A multi-disciplinary team (MDT) should be formed based on the individualized 3D model and the results of clinical examinations; liver surgeons undertake the main tasks, assisted by the departments of hepatology, oncology, endoscopy, interventional therapy and radiotherapy.	+2
15	The consistency between preoperative 3D models and intraoperative conditions (lesions, vascular variance and range of hepatectomy) should be assessed.	+3 (completely consistent): +2 (basically consistent): -1 (inconsistent)
16	The volume of the virtual resected liver with that of the actual resected liver (reference standard is intraoperative dewatering method) should be compared. The volume error (<5%) is completely consistent, the volume error (< 10%) is basically consistent, and the volume error (>10%) is inconsistent.	+3 (completely consistent); +2 (basically consistent); -1 (inconsistent)
Total score (24, 100%)		

For patients with ICG R15 ⩽7%, good imaging results can be achieved when ICG is administered more than 48 h before the operation, and preferably over 5 days preoperatively. For patients with ICG R15 >7%, ICG should be administered over 6 days before the operation to ensure good results of intraoperative fluorescence imaging[22]. More specific recommendations are listed in Tab.2.

3.3 Near infrared light detection

ICG molecular fluorescence imaging system mainly includes near-infrared excitation light source, high-sensitivity near-infrared fluorescence video camera, and a computer image processing system. Typically, the procedures of intraoperative operation are as follows:

(1) After the liver is fully dissociated, the surgical light in the operating zone is turned off. Under the near-infrared excitation light source, the liver and other abdominal organs are scanned using a near-infrared fluorescence video camera at a proper distance (according to the model type);

(2) With real-time localization of the hepatic tumor, the hepatic precutting line is calibrated according to the distribution of the fluorescence signal;

(3) During anatomical hepatectomy, positive or negative display method is used to guide liver segmentation;

(4) After hepatectomy, ICG fluorescence on the residual liver and the resected tissues is detected;

(5) Routine pathological examination of the resected

Tab.2 Dosage and administration methods of indocyanine green

Purpose	Injection time	Administration method	Injection dosage
Identification and location of tumors	Based on ICG R15	IV	0.25-0.5 mg/kg
Definition of tumor boundaries	Based on ICG R15	IV	0.25-0.5 mg/kg
Detection of residual liver	Based on ICG R15	IV	0.25-0.5 mg/kg
Hepatic segmentation (Negative Display Method)	Intraoperative	IV	1 mL (2.5 mg/mL)
Hepatic segmentation (Positive Display Method)	Intraoperative	PV	0.1 mL (2.5 mg/mL) mixed with 5.0 mL indigo carmine
Hepatic segmentation (Experimental phase)	Intraoperative	IA	1 mL (1 mg/mL)
Delineation of hepatectomy line (NAH)	Preoperative	IV	0.25-0.5 mg/kg
Delineation of hepatectomy line (AH)	Intraoperative	IV/PV	Refer to hepatic segmentation dose
Detection of Biliary Leakage in Liver Section	Intraoperative	Transcystic duct	5-10 mL (2.5 mg/mL)
Living donor liver transplantation (Biliary reconstruction)	Intraoperative	Transcystic duct	2 mL (2.5 mg/mL)
Living donor liver transplantation (Revascularization)	Intraoperative	IV	1.5 mL (2.5 mg/mL)

IV: Injection through peripheral vein; NAH: Nonanatomical hepatectomy; AH: Anatomical hepatectomy; PV: Injection through portal vein of the targeted hepatic segment; IA: Injection through femoral artery puncture surpassing selective hepatic segment artery.

tissues is performed.

3.4 Adverse reactions

The incidence of adverse reactions is less than 0.01%. The instructions for drug usage should be strictly followed[22].
Recommendation: ICG should be sufficiently dissolved with sterile water for injection to avoid potential adverse reactions. The timing, route of administration, and dosage of ICG injection vary according to different purposes (Strong recommendation).

4. Clinical application of 3D visualization and virtual reality technologies

A 3D visualization model allows for observation of the size, site, and morphology of liver tumors from different angles, of the anatomic variations of the celiac vasculature, and of the spatial relation between the tumor and the major blood vessels in the liver. Individualized liver segmentation and liver volume calculation can be used to guide precise hepatectomy. The 3D visualization model can be compared with the actual surgical findings in real time to allow synchronous adjustment of the anatomical position of the 3D model as well as the identification and localization of the key pipeline[23]; at the same time, virtual reality studies can be carried out (Fig.1).
Recommendation: With 3D visualization and virtual reality technologies, accurate diagnosis and safety assessment of liver tumors is possible before the operation, and the tumors and important blood vessels can be identified and localized during the operation to facilitate a precise operation (Strong recommendation).

5. Clinical applications of ICG molecular fluorescence imaging

5.1 Assessment of differentiation of primary hepatic carcinoma

Poorly differentiated hepatic carcinoma tissue has a low ICG uptake to result in a low intensity of fluorescence signals in the tumor foci. But in the adjacent normal liver tissues, the compression by the tumor causes delayed excretion of ICG and hence annular fluorescence
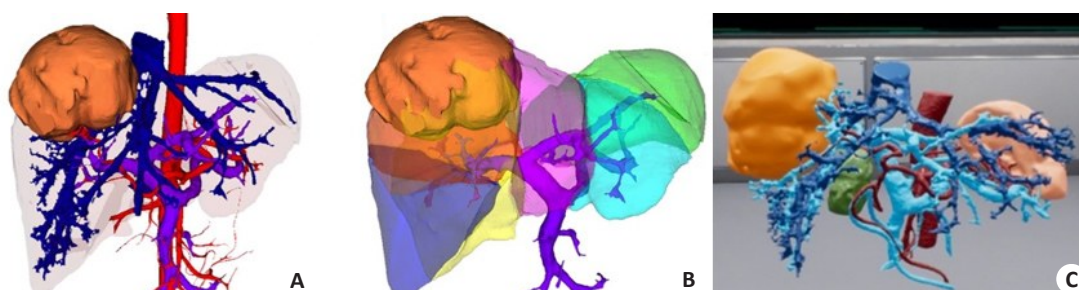

Fig.1 3D visualization evaluation. **A**: 3DVT to display intrahepatic tumors and abdominal vascular system; **B**: 3D visualization of liver segments; **C**: Virtual reality reconstruction model.

signals surrounding the tumor tissues. In well differentiated hepatic carcinoma tissues that have a relatively high ICG uptake, the biliary tract excretory function is impaired and thus persistent fluorescence can be detected for a longtime with full fluorescence signals. Some of the cells in moderately differentiated hepatic carcinoma tissues are not capable of ICG uptake, and the tumors often emit partial fluorescence signals [24].

Recommendation: The degree of differentiation of primary hepatic carcinoma can be preliminarily determined according to the intraoperative fluorescence signal characteristics of the liver tumor combined with rapid intraoperative pathological examination (Weak recommendation).

5.2 ICG molecular fluorescence imaging in treatment of primary liver cancer

The postoperative recurrence rate of primary hepatic carcinoma remains high, possibly due to the presence of microdisseminated tumor foci or multiple sources of tumor cells before the operation. In cases with obvious liver cirrhosis, the preoperative diagnosis and intraoperative detection of the microfoci of hepatocellular carcinoma are difficult [25]. Studies have suggested that some primary hepatic carcinoma foci can not be detected with preoperatively using other imaging modalities or intraoperatively with B ultrasound, naked eye, or hand touch, and can only be identified by ICG molecular fluorescence imaging. The technology is capable of detecting primary hepatic carcinoma foci with a minimum diameter as small as 2 mm [2, 26].

5.2.1 Definition of left and right hepatic boundary

Currently the methods for labeling the left and right half liver include blocking the hemihepatic blood flow to observe the ischemic line on the surface of the liver, and injecting methylene blue into the portal vein with ultrasound guidance. But the ischemic line can sometimes be unclear, and the injected dyes are easily washed out. By comparison, ICG can provide sustained staining of the liver for a long time, and the staining is not confined to the surface of the liver to achieve a stereotatic staining effect. ICG can clearly define the left and right hepatic boundary during the operation and assist navigation operation. In the actual operation, the left and right hemihepatic boundary defined by ICG molecular fluorescence imaging is regular in a few cases, and irregular in most cases, shown as humped and mapped lines (Fig.2).
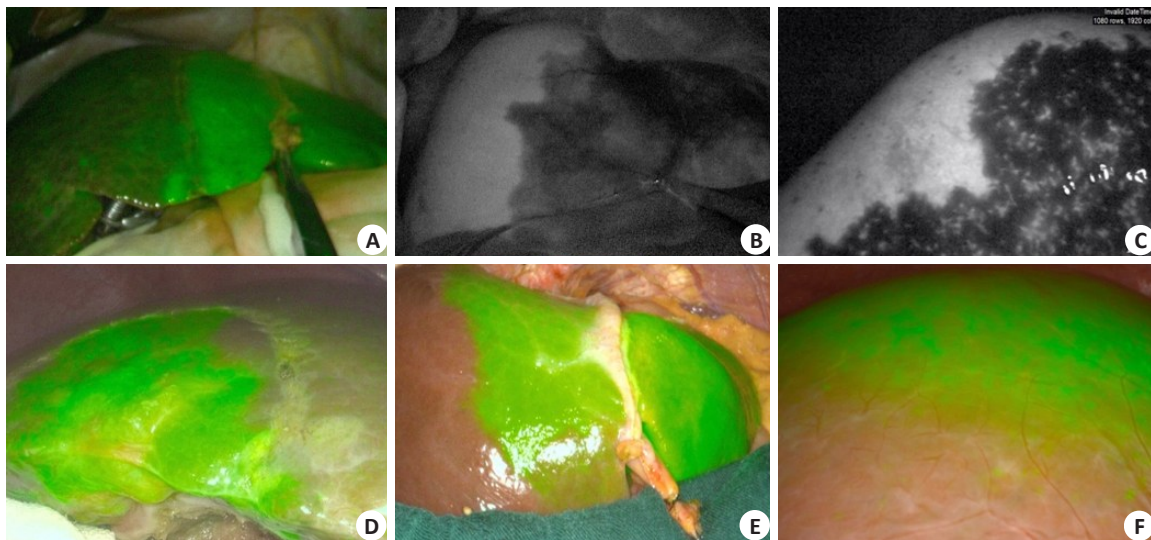
Recommendation: For patients undergoing anatomical

Fig.2 Definition of left and right hepatic boundary by ICG molecular fluorescence imaging. **A**: The left and right hepatic boundary is linear; **B**-**C**: The left and right hepatic boundary is humped; **D**-**E**: The left and right hepatic boundary is irregular; **F**: The left and right hepatic boundary is unclear, considering existence of vascular communicating branches.

hepatectomy, ICG molecular fluorescence imaging can achieve left and right hemiliver staining to allow dynamic stereoscopic observation during the operation. The scope of hepatectomy can be adjusted and liver resection can be guided in real time according to the fluorescence boundary of the liver parenchyma (Strong recommendation).

5.2.2 Detection of residual tumors and minimal lesions using ICG molecular fluorescence imaging

CT and magnetic resonance imaging (MRI) are often used to identify small liver tumors before the operation, and ultrasound is used to locate the tumors during the operation. But for small liver tumors less than 1.0 cm, especially in cases with cirrhosis, these imaging modalities have a low sensitivity and the intraoperative localization is inconvenient [27]. Therefore, the small lesions on the surface of the liver or residual lesions on the incision margin still remain blind spots in conventional detection methods [28]. ICG molecular fluorescence imaging has a high sensitivity for detecting small lesions on the superficial surface of the liver or residual lesions on the incision margin less than 1 cm, and can detect the small tumor foci that are not found by CT or MRI before the operation (Fig.3).
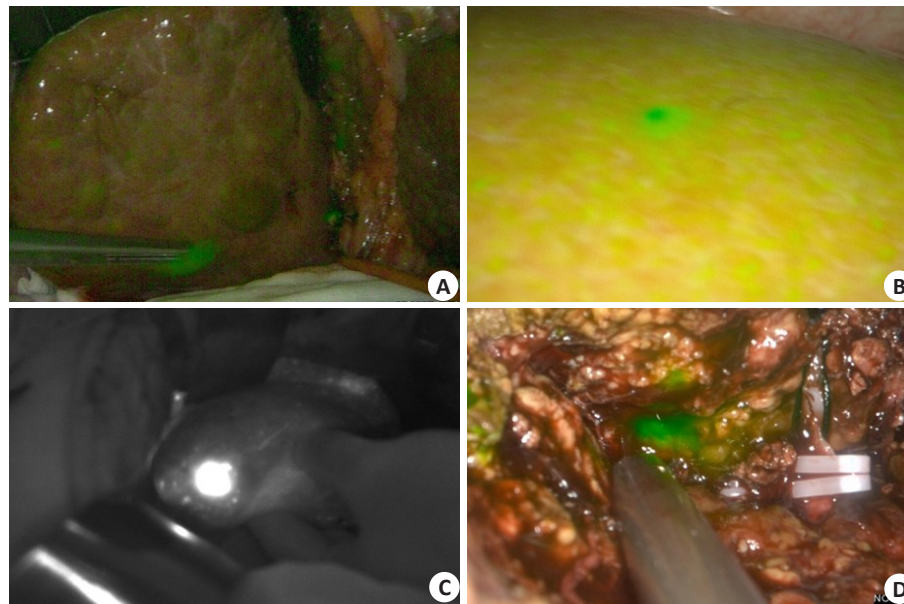
Fig.3 Intraoperative detection of small liver tumors by ICG molecular fluorescence imaging. **A**-**C**: Detection of small liver tumors on the liver surface; **D**: Detection of deep small liver tumors after incision of liver parenchyma.

Recommendation: ICG molecular fluorescence imaging can be used to detect the liver tumors during the operation by identifying high-intensity fluorescence signal. Its combination with intraoperative ultrasound and rapid pathological examination can help in resecting suspicious tumor foci (Strong recommendation).

5.2.3 Intraoperative determination of liver tumor boundaries

Accurate definition of the tumor boundary is key to hepatectomy. Currently the boundary of the tumors is determined mainly by intraoperative observation, palpation and intraoperative ultrasound. A too small resection range can fail to achieve R0 resection, and an excessive range of resection is associated increased risks of vascular injury and postoperative liver failure. Capable of showing pathological changes at the cellular and molecular levels in living organisms, ICG molecular fluorescence imaging can recognize and accurately define the boundary of tumors and the extent of hepatectomy at the cellular level. In nonanatomical hepatectomy with ICG injection through the peripheral vein before the operation, the tumor boundary can be defined by detecting the fluorescence, and the range of hepatectomy can be determined with a precision of at least 1 cm from the tumor. For anatomical hepatectomy, intraoperative positive or negative display methods can be used to define the hepatic regions or hepatic segments to be resected, and precise hepatectomy can be performed (Fig.4). The results of meta-analysis confirm that ICG molecular fluorescence imaging can significantly improve the negative rate of the incision margins.

Recommendation: ICG molecular fluorescence imaging combined with 3DVT can be used to delineate the tumor boundary and the range of hepatectomy during the operation (Strong recommendation).

5.2.4 Detection of biliary leakage after hepatectomy

Bile leakage after hepatectomy is one of the important causes of abdominal infection, hepatic failure and even death, and its incidence ranged from 4% to 9.8% [29-32]. The key to reducing the incidence of bile leakage is the timely detection and repair of bile leakage during the operation. At present, the detection of bile leakage relies mainly on injection of methylene blue solution into the cystic duct; but the injection of the dye can also stain the surrounding liver tissues, which makes it difficult to accurately locate bile leakage. Intraoperative cholangiography, as the gold standard for detecting bile leakage, is not the optimal method because of the radiation exposure and complex operation. In recent years, angiography based on ICG molecular fluorescence imaging technology has been used to evaluate the patency of blood vessels. As bile contains proteins that can bind to ICG, bile leakage can be identified by injecting ICG through the ductus cysticus, temporarily blocking the common bile duct and detection of the fluorescence signals (Fig.5)[33]. Some studies suggest that the detection of bile leakage after hepatectomy using ICG molecular fluorescence imaging, compared with the conventional methods, can significantly reduce the incidence of postoperative bile leakage [34]. In addition, this technique also helps to prevent hepatic cyst and bile leakage after hepatic cystadenoma excision[35].

Recommendation: ICG molecular fluorescence imaging can effectively detect bile leakage after hepatectomy (Weak recommendation).
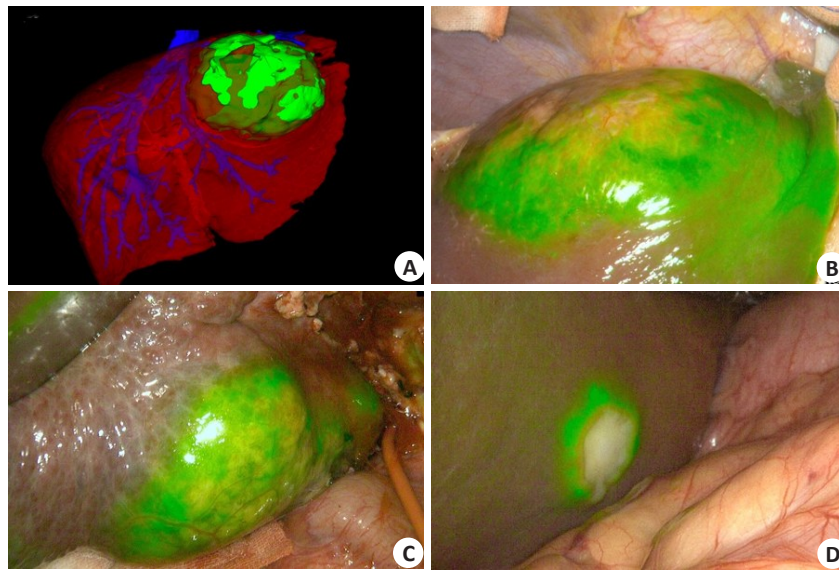
5.2.5 Colorectal liver metastases

Fig.4 Intraoperative determination of tumor boundary. **A**-**B**: Intraoperative ICG molecular fluorescence imaging combined with 3DVT to determine the tumor boundary; **C**-**D**: ICG molecular fluorescence imaging to determine the tumor boundary.
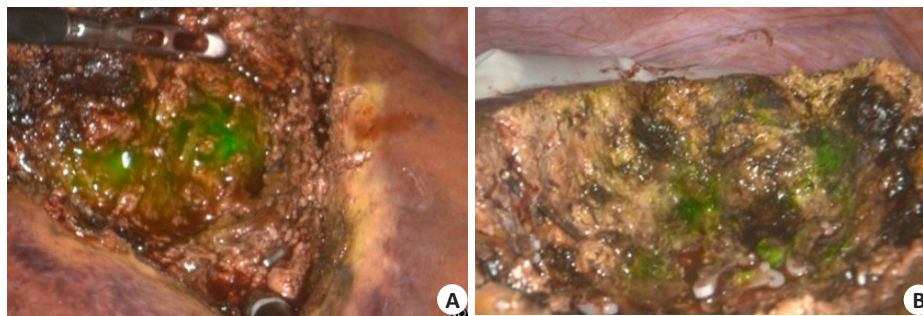

Fig.5 Detection of ICG molecular fluorescence imaging fluorescence for residues in hepatic sections. **A**: Fluorescence residues in liver section; **B**: No fluorescence is detected after suture and ligation.

Liver is the hematogenous metastasis organ of malignant tumors, and hepatic metastases of colorectal cancer are common. Radical excision of intrahepatic metastatic carcinoma is recommended on the premise that the primary cancer foci have been or can be radically resected, and the residual liver has an adequate compensatory function [36-37]. However, the conventional modalities including CT, MRI, and intraoperative B ultrasound often fail to detect small cancer foci, which makes a complete resection difficult for hepatic metastasis. The hepatic metastatic carcinoma tissues do not possess hepatocyte functions, and generally show annular fluorescence around the tumor tissue in ICG molecular fluorescence imaging. Studies show that for metastatic cancerous nodes, preoperative imaging examinations and intraoperative B ultrasound all have far lower detection rates than ICG molecular fluorescence imaging. The minimum diameter of the nodes detectable by ICG molecular fluorescence imaging is 1.5 mm [38-39].

Recommendation: For patients with hepatic metastases of colorectal cancer, when the primary cancer foci have been radically resected and the residual liver is evaluated to have adequate compensatory function, the metastatic cancer foci can be resected with assistance by ICG fluorescence imaging (Weak recommendation).

5.2.6 Extrahepatic metastases of primary hepatic carcinoma

For extrahepatic metastases of primary liver cancer, the detectability of the fluorescent signals may differ in different metastatic organs, which deserves clinical attention [5, 40].

Recommendation: ICG molecular fluorescence imaging can be used for identification and localization of extrahepatic metastatic tumor of primary hepatic carcinoma (Weak recommendation).

5.3 Preliminary identification of tumor origin related with the liver

Peritoneal space-occupying lesions with unknown origins are common. For instance, the tumors with adhesion to or compressing the liver can be easily misdiagnosed as liver cancer by imaging examinations when they are located in the left hemiliver, in the gap

between the liver and stomach or in the rear of the liver. Intraoperative rapid pathological examination is of great importance in determining the surgical approach for such patients. However, misdiagnosis and missed diagnosis still exist in the examination[41]. The tumors of a nonhepatic origin do not show fluorescence retention due to their low ICG uptake and metabolism, both in the tumors and in the surrounding tissues. When ICG is injected preoperatively through the peripheral vein and extensive metabolism is eliminated, there is only a low possibility that the focus is derived from the liver when no fluorescence was detected intraoperatively in the tumor and the surrounding tissues.

Recommendation: ICG molecular fluorescence imaging can be used as a supplementary means for tumor identification, and the combination with preoperative 3D visualization evaluation and intraoperative rapid pathological examination can improve the accuracy of intraoperative diagnosis (Weak recommendation).

5.4 Ultrasound-guided ICG fluorescence imaging of portal vein puncture

Two methods are commonly used to demarcate the hepatic segments in intraoperative ICG molecular fluorescence imaging, namely the positive display methodand the negative display method [20, 42]. In the positive display method, the portal vein of the hepatic segment to be resected is identified by intraoperative B ultrasound and 3D visualization model, ICG solution is extracted using a fine puncture needle and injected into the target portal vein branch, and ICG molecular fluorescence detection is carried out to display the target hepatic segment. The fluorescence signal of positive display is strong, but the technical difficulty is greater than that of negative display method[43-44]. In the negative display method, the portal vein of the target hepatic segment is separated and ligated, ICG solution is injected through the peripheral vein, and ICG molecular fluorescence detection is carried out to display the hepatic segment to be reserved. Negative display method is usually appropriate for hepatic segments with easily exposed portal vein branch. The disadvantage is its low concentration of ICG accumulation and hence the relatively weak fluorescence signal. Studies show that using ICG molecular fluorescence imaging, the success rate of segmentation can reach 95.8%. This imaging modality can accurately display the boundaries of the hepatic segments on the surface of the liver and also shows the fluorescence boundaries on the cross-section of the liver; it has a strong effect of visualized segmentation on the hepatic surface with 3D staining of the hepatic parenchyma[4].

In anatomical hepatectomy, the Glisson pedicle of segment Ⅷ varies greatly and its location is deep. It is difficult and time-consuming to dissect and ligate the Glisson pedicle of segment Ⅷ from the porta hepatis, so that negative staining is not easy to implement. Intraoperative ultrasound combined with 3D visualization-guided puncture of the portal vein branches in segment Ⅷ is easier to achieve (Fig.6).

Segment Ⅶ is located in the upper segment of the right posterior lobe. Most of the portal veins supplying segment Ⅶ have one branch and sometimes have another lateral branch. Therefore, the success rate is high for intraoperative ultrasound-guided portal vein puncture by ICG positive staining (Fig.7).

Glisson pedicle of the segment Ⅵ is easily dissected in the Rouviere sulcus, so that negative staining is easy to implement. About 76% of the portal veins that dominates the segment Ⅵ have one branch, and therefore intraoperative ultrasound-guided puncture of the portal vein can also be used for positive staining (Fig.8).

The segment Ⅴ is located in the lower right anterior segment. The extrathecal segregation and dissection of the right anterior Glisson pedicle dominating the segment Ⅴ can be carried out by lowering the hilar plate, so that the negative staining method is easy to implement. For those who are skilled in portal vein puncture, positive staining with portal vein puncture can also be used (Fig.9).

The main portal vein branches in the segment Ⅳ are the upper and lower branches, but positive staining via portal vein puncture may not cover all the segment Ⅳ or the staining is not uniform. If the Glisson pedicle of the section Ⅳ is slowly separated along the right side of the ligamentum teres hepatis and sagittal segment, multiple branches can be seen entering the segment Ⅳ. Therefore, satisfactory results can be obtained by negative staining after ligation and cutting of all the branches of the segment Ⅳ and defining the ischemic line of the segment Ⅳ (Fig.10).

The Glisson pedicle of the segment Ⅲ is superficial and easy to separate on the left side of the sagittal region. Negative staining is often used, which is simple and feasible. Segment Ⅲ is usually dominated by only one portal vein, and intraoperative ultrasound-guided positive staining of portal vein is also easy to implement (Fig.11).

The Glisson pedicle of the segment Ⅱ is deep on the left side of the sagittal region. Although the corresponding branches can be dissected from the visceral surface of the left lateral lobe into the liver, the segment Ⅱ can be delineated by negative staining method. Because the segment Ⅱ is usually dominated by only one portal vein, the success rate of positive staining of ICG guided by ultrasound is high and time-saving (Fig.12).

The branches of the portal vein in the segment Ⅰ are superficial and thin, and ultrasound-guided puncture is not easy. Therefore, the Glisson pedicle of the segment Ⅰ is usually dissected and negative stained after clipping can be performed (Fig.13).

Recommendation: Intraoperative positive display method or negative display method can be used to produce fluorescence signal in the target hepatic region or hepatic segment to assist anatomical hepatectomy (Strong recommendation).

5.5 Living donor liver transplantation

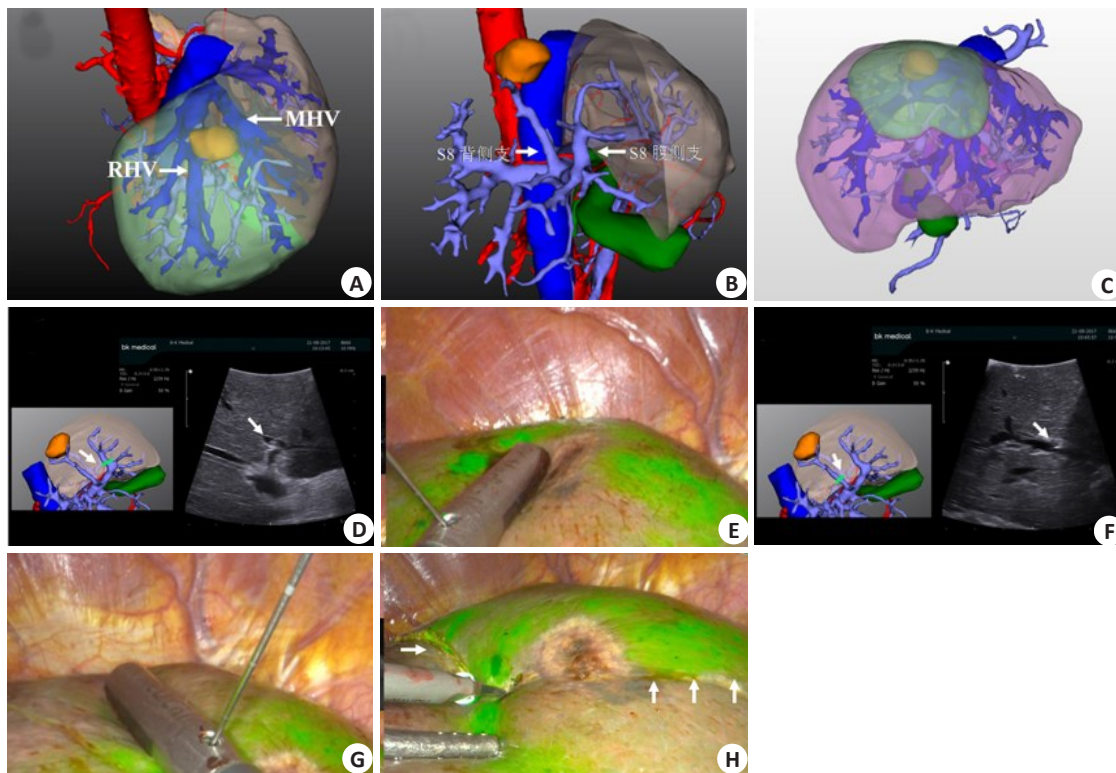In living donor liver transplantation, ICG molecular

Fig.6 Portal vein puncture of segment VIII staining guided by laparoscopic ultrasound combined with 3DVT. **A**: 3D visualization reconstruction of liver; **B**: 3D visualization showing portal vein branches of segment VIII; **C**: 3D visualization showing segment VIII portal vein branches watershed (green area); **D**: laparoscopic ultrasound combined with 3DVT to guide ventral portal vein branch puncture of segment VIII (arrow); **E**: ICG fluorescence staining after successful puncture of ventral portal vein branch of segment VIII; **F**: Laparoscopic ultrasound combined with 3DVT to guide dorsal portal vein branch puncture of segment VIII (arrow); **G**: ICG fluorescence staining after successful puncture of dorsal portal vein branch of segment VIII; **H**: Resection line is labeled along the boundary of the segment VIII with indocyanine green fluorescence staining.
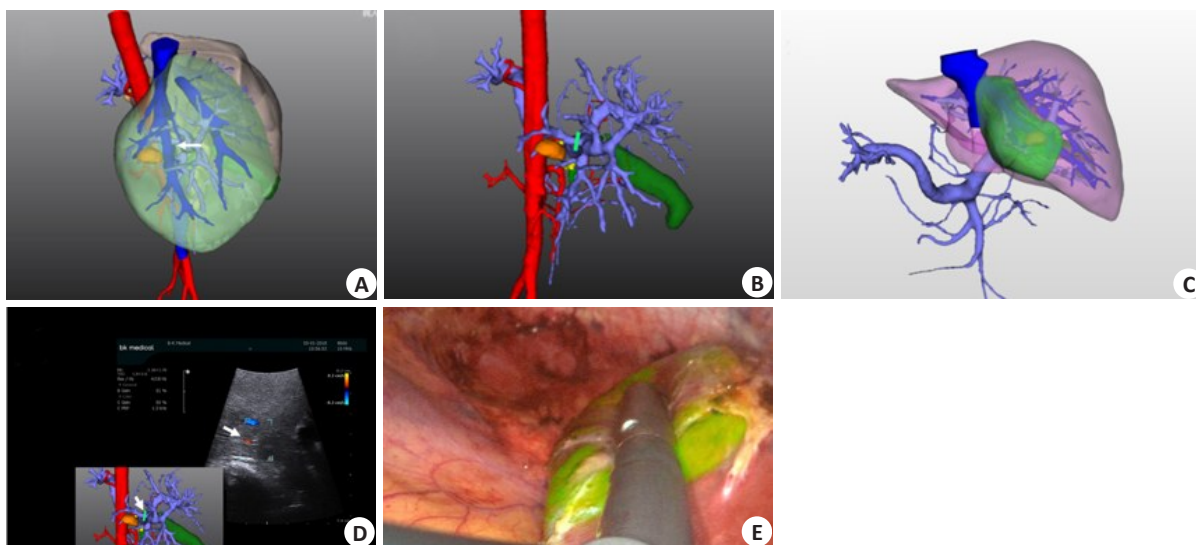

Fig.7 Portal vein puncture of segment VII staining guided by laparoscopic ultrasound combined with 3DVT. **A**: 3D visualization reconstruction of liver; **B**: 3D visualization showing segment VII portal vein branches, drawing up portal vein puncture point; **C**: 3D visualization showing segment VII portal vein branch watershed; **D**: Laparoscopic ultrasonography combined with 3D visualization to guide portal vein branch puncture of segment VII; **E**: ICG fluorescent staining of hepatic segment VII after successful portal vein puncture and injection.
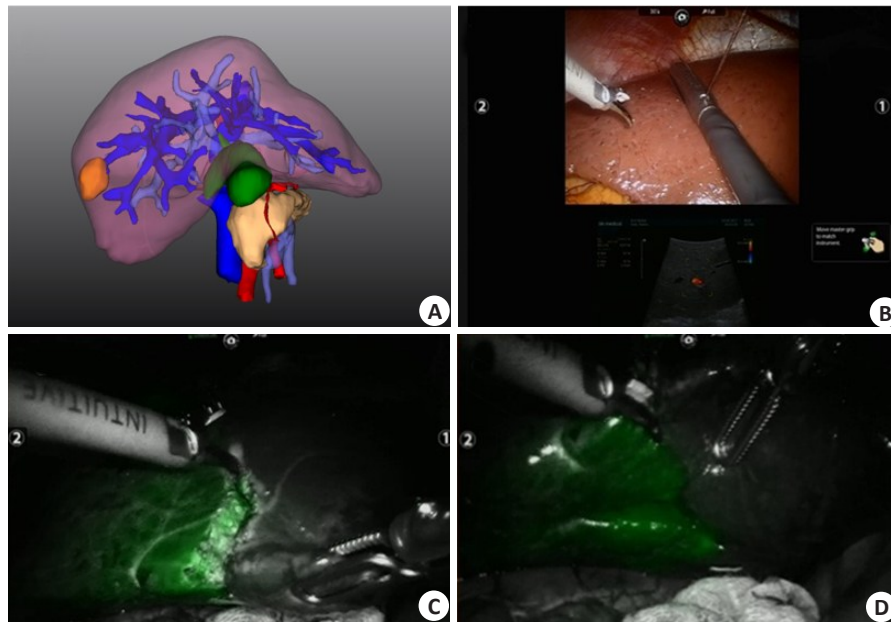
Fig.8 Portal vein puncture of segment VI staining guided by laparoscopic ultrasound combined with 3DVT. **A**: 3D visualization showing the portal vein branches of segment VI; **B**: Laparoscopic ultrasound combined with 3DVT to guide the portal vein puncture of segment VI; **C**: ICG fluorescence staining of segment VI (diaphragm view) after successful portal vein puncture; **D**: ICG fluorescence staining of segment VI (visceral view) after successful portal vein puncture.
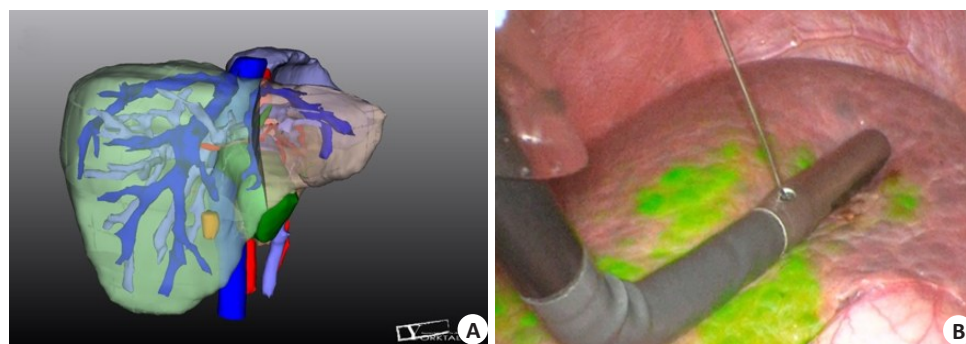

Fig.9 Portal vein puncture of segment V staining guided by laparoscopic ultrasound combined with 3DVT. **A**: 3D visualization showing segment V portal vein branches; **B**: Portal vein branch puncture of segment V is guided by laparoscopic ultrasound combined with 3DVT.
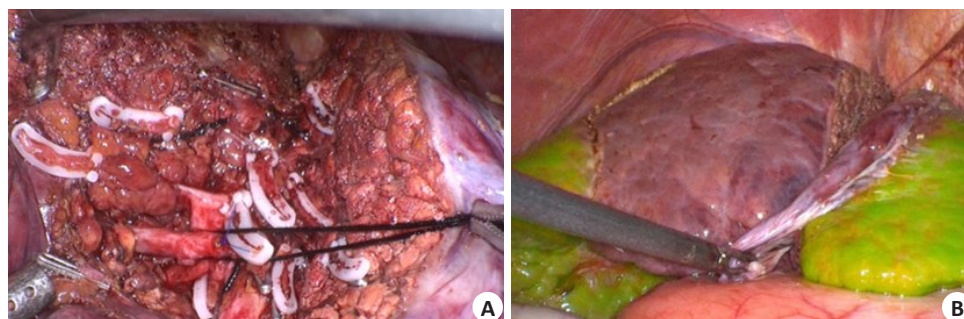

Fig.10 Negative staining of segment IV. **A**: Glisson pedicle of section IV is gradually separated and resected along the right side of the ligamentum teres hepatis and sagittal segment; **B**: After ischemic line of segment IV being defined, ICG fluorescence staining is carried out using the negative staining method.
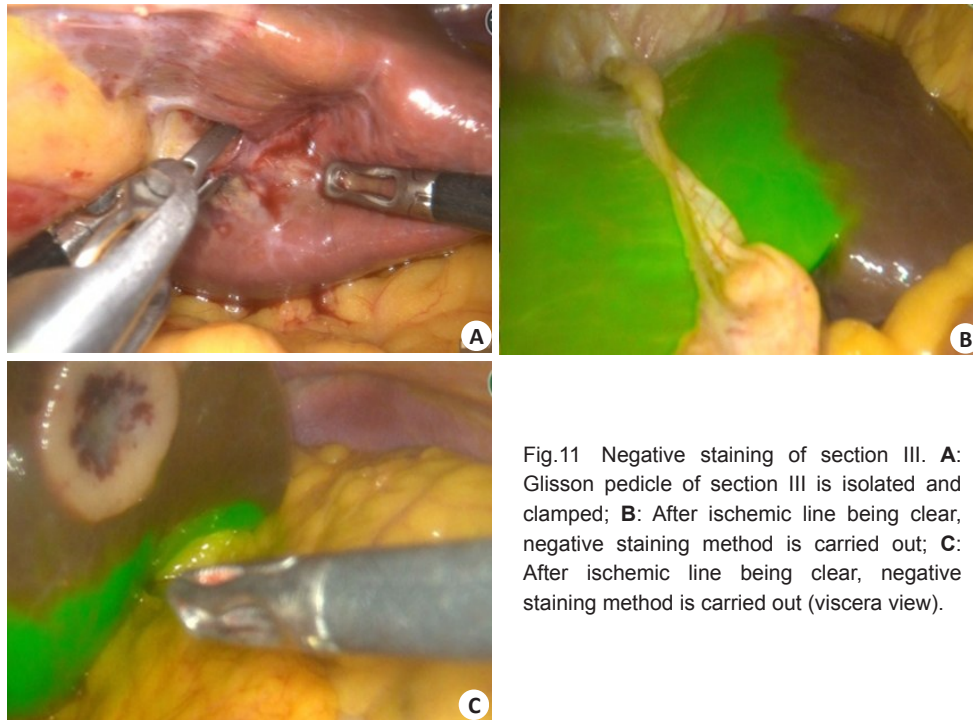
Fig.11 Negative staining of section III. **A**: Glisson pedicle of section III is isolated and clamped; **B**: After ischemic line being clear, negative staining method is carried out; **C**: After ischemic line being clear, negative staining method is carried out (viscera view).
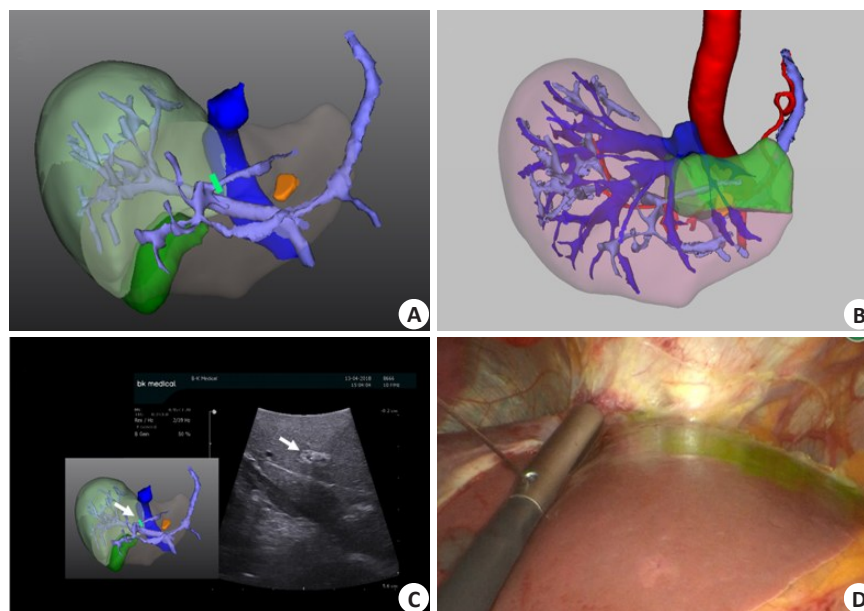

Fig.12 Portal vein puncture of segment II staining guided by laparoscopic ultrasound combined with 3DVT. **A**: 3D visualization showing segment II portal vein branches; **B**: 3D visualization showing portal vein branches watershed of segment II (green area); **C**: Portal vein branch puncture of segment II is guided by laparoscopic ultrasound combined with 3DVT; **D**: ICG fluorescence staining of segment II after successful portal vein puncture.

fluorescence imaging is used mainly for cholangiography and for assessment of vascular patency and liver function recovery. In cholangiography, ICG is injected through the cystic gall duct, and clear biliary ductal anatomic images can be obtained with ICG molecular fluorescence imaging, which helps to accurately determine the donor liver preresection line and the bile duct cut point, and to guide the biliary tract reconstruction. The use of ICG molecular fluorescence imaging helps to reduce the incidence of bile leakage, bile duct stenosis, and other complications as well[21, 43]. As ICG can rapidly bind to plasma proteins after intravenous injection and is distributed in systemic blood vessels, ICG molecular fluorescence imaging can be used for angiography; It can also be used to verify the normal bile production by the transplanted liver graft, indicated by the detection of the extrahepatic bile duct on ICG near-infrared light image following injection of ICG through the peripheral vein during operation[44].

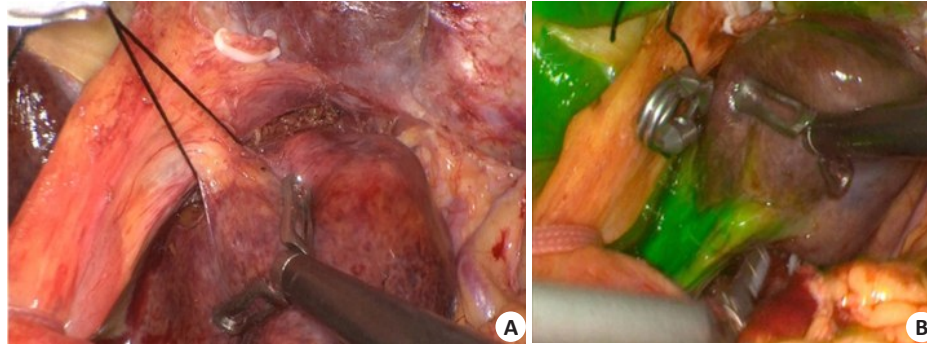***Recommendation***: In living donor liver transplantation, ICG

Fig.13 Negative staining in segment I. **A**: Dissection of Glisson sheath in segment I; **B**: Negative staining of segment I after clipping.

molecular fluorescence imaging can be used to carry out cholangiography and guide biliary tract dissociation and reconstruction; it also allows functional assessment of the liver graft during the operation in different types of liver transplantation (Weak recommendation).

6. DISCUSSION

At present, ICG molecular fluorescence imaging has two major technical limitations: its low sensitivity for detecting deep nodules and the high false-positive rate for hepatic nodules. Due to the limited ability of near-infrared light to penetrate human tissues, the fluorescence signals emitted by ICG can only penetrate 10 mm of liver parenchyma [24]. This is remedied only by dynamic detection of ICG molecular fluorescence on the hepatic section during hepatectomy, and the combination of intraoperative ultrasound and intraoperative rapid pathological examination. Its high false-positive rate for detecting hepatic nodules, especially in patients with hepatic cirrhosis, results from the low fluorescence contrast ratio between the tumor tissue and the adjacent tissues [45]. The detection rate and the characteristics of false-positive foci need to be further investigated by further case studies with large sample sizes. In addition, attention should be paid to the perioperative protection of the liver function and immune function, the surgical techniques and the performance of ICG molecular fluorescence imaging [46-47].

Computer-assisted ICG molecular fluorescence imaging technique provides a new digital medical technology for the diagnosis and surgical navigation for liver tumors. ICG-targeted optical molecular imaging probes for diagnostic and therapeutic purposes have received increasing attention. It is believed that with the continuous development of its clinical application and technical innovation, this technology will continue to evolve to better facilitate precise diagnosis and treatment of liver tumors.

Validated by: LAU Wanyee
Directors of the Committee: FANG Chihua, JIANG Hongchi, LIANG Lijian
Participants: BAO Susu (School of Computer Science of South China Normal University), BIE Ping (the First Hospital affiliated to AMU), CHEN Yajin (Sun Yat-Sen Memorial Hospital, Sun Yat-set University), CHEN Guihua (Third Affiliated Hospital, Sun Yat-set University), CHEN Rufu (Sun Yat-sen Memorial Hospital, Sun Yat-set University), CAI Xiujun (Sir Run-Run Shaw Hospital, Zhejiang University), CAI Xiangjun (General Hospital of the Northern War Zone of the Chinese People's Liberation Army), CHENG Shuqun (Eastern Hepatobiliary Surgery Hospital, Naval Medical University), DONG Ming (First Hospital of china medical university), DAI Chaoliu (Sheng Jing Hospital of China Medical University), FANG Chihua (Zhujiang Hospital, Southern Medical University), FAN Jia (Zhongshan Hospital, Fudan University), FAN Haining (Qinghai University Affiliated Hospital), GUO Wei (Beijing Friendship Hospital, Capital Medical University), GENG Xiaoping (Second Hospital of Anhui Medical University), HE Yu (The First Hospital Affiliated to AMU), LI Yumin (Lanzhou university), LI Zongfang (Second Affiliated Hospital of Xi´an Jiaotong University), JIA Weidong (First Affiliated Hospital of University of Science and Technology of China), JIANG Xiaoqing (Eastern Hepatobiliary Surgery Hospital, Naval Medical University), JIANG Kewei (Peking University People's Hospital), JIANG Hongchi (First Affiliated Hospital of Harbin Medical College), JIAN Zhixiang (Guangdong Provincial People's Hospital), JIANG Yi (Hospital of The Joint Logistics Team), KONG Dexing (School of Mathematical Scinence, Zhejiang University), LAU Wanyee (Faculty of Medicine, The Chinese University of Hong Kong), LIU Jun (First Affiliated Hospital of Xi'an Jiaotong University), LIU Lianxing (Department of Hepatobiliary Surgery, the First Affiliated Hospital of USTC,), LIU Jingfeng (Mengchao Hepatobiliary Hospital of Fujian Medical University), LIU Jingang (Fourth Affiliated Hospital of China Medical university), LIU Chao (Sun Yat-san Memorial Hospital of San Yat-sun University), LIU Yingbin (Xinhua Hospital Affiliated to Shanghai Jiao Tong University School of Medicine), LIANG Lijian (First Affiliated Hospital, Sun Yat-Sen University,), LIANG Xiao (Sir Run-Run Shaw Hospital, Zhejiang University), LU Qiping (Department of General Surgery, General Hospital of Central Theater Command), OU Jinrui (Guangdong Provincial People's Hospital), PENG Baogang (First Affiliated Hospital, Sun Yat-Sen University), QUAN Zhiwei, QI Xiaolong (First Hospital of Lanzhou University), QIN Lunxiu (Huashan Hospital, Fudan University), QIN Renyi (Tongji Hospital, Tongji Medical

College, Huazhong University of Science and Technology), QUAN Zhiwei (Xinhua Hospital Affiliated to Shanghai Jiao tong University School of Medicine), SUN Bei (First Affiliated Hospital of Harbin Medical University), SUN Chengyi (Affiliated Hospital of Guizhou Medical University), SUN Shijie (Yantai YuHuangDing Hospital), SHEN Feng (Eastern Hepatobiliary Surgery Hospital, Naval Medical University), TIAN Jie (Institute of Automation, Chinese Academy of Sciences), TIAN Liguo (Editorial Department of Chinese Journal of Practical Surgery), TANG Zhaohui (Xinhua Hospital Affiliated to Shanghai Jiao Tong University School of Medicine), WANG Jian (Renji Hospital, shanghai jiaotong University School of Medicine), WANG Jianming (Tongji Hospital. Tongji Medical College. Huazhong University of Science and Technology), WANG Xiaoyin (Zhongshan Hospital, Fudan University), WANG Huaizhi (First Hospital Affiliated to AMU), WANG Wei (Huadong Hospital, Fudan University), WANG Hongguang (Chinese PLA General Hospital), WEN Hao (First affiliated hospital of Xinjiang Medical University), YANG Yinmo (Peking University First Hospital), YANG Yang (Third Affiliated Hospital, Sun Yat-Set University), YIN Xiaoyu (First Affiliated Hospital of Sun Yat- Sen university), YIN Xinmin (Hunan Provincial People's Hospital), YUAN Yufeng (Zhongnan Hospital Affiliated to Wuhan University), ZHANG Shaoxiang (Army Medical University), ZHANG Bixiang (Tongji Hospital, Tongji Medical College. Huazhong University of Science and Technology), ZHANG Yongjie (Eastern Hepatobiliary Surgery Hospital, Naval Medical University), ZHANG Xuewen (China-Japan Union Hospital, Jilin University), ZHANG Taiping (Peking Union Medical College Hospital), ZHOU Weiping (Eastern Hepatobiliary Surgery Hospital, Naval Medical University), ZHOU Jie (Nanfang Hospital, Southern Medical University), ZHONG Lin (The First People's Hospital Affiliated to Shanghai Jiao tong University), ZHI Xuting (Qilu Hospital of Shandong University)

Byliners: FANG Chihua, LU Qiping, LAU Wanyee

REFERENCES

[1] Landsman ML, Kwant G, Mook GA, et al. Light-absorbing properties, stability, and spectral stabilization of indocyanine green [J]. J Appl Physiol, 1976, 40(4): 575-83.

[2] Ishizawa T, Fukushima N, Shibahara J, et al. Real-time identification of liver cancers by using indocyanine green fluorescent imaging [J]. Cancer, 2009, 115(11): 2491-504.

[3] Morita Y, Sakaguchi T, Unno N, et al. Detection of hepatocellular carcinomas with near-infrared fluorescence imaging using indocyanine green: its usefulness and limitation [J]. Int J Clin Oncol, 2013, 18(2): 232-41.

[4] Inoue Y, Arita J, Sakamoto T, et al. Anatomical liver resections guided by 3-dimensional parenchymal staining using fusion indocyanine green fluorescence imaging[J]. Ann Surg, 2015, 262(1): 105-11.

[5] Satou S, Ishizawa T, Masuda K, et al. Indocyanine green fluorescent imaging for detecting extrahepatic metastasis of hepatocellular carcinoma[J]. J Gastroenterol, 2013, 48(10): 1136-43.

[6] Tanaka T, Takatsuki M, Hidaka M, et al. Is a fluorescence navigation system with indocyanine green effective enough to detect liver malignancies [J]. J Hepatobiliary Pancreat Sci, 2014, 21(3): 199-204.

[7] Yang J, Tao HS, Cai W, et al. Accuracy of actual resected liver volume in anatomical liver resections guided by 3-dimensional parenchymal staining using fusion indocyanine green fluorescence imaging[J]. J Surg Oncol. 2018. 118(7): 1081-7.

[8] Guyatt GH, Oxman AD, Vist GE, et al. GRADE: an emerging consensus on rating quality of evidence and strength of recommendation [J]. BMJ, 2008, 336(7650): 924-6.

[9] Guyatt GH, Oxman AD, Schunemann HJ, et al. GRADE guidelines: a new series of articles in the Journal of Clinical Epidemiology[J]. J Clin Epidemiol, 2011, 64(4): 380-2.

[10] Meerpohl J J, Langer G, Perleth M, et al. GRADE guidelines: 3. Rating the quality of evidence (confidence in the estimates of effect) [J]. Z Evid Fortbild Qual Gesundhwes, 2012, 106(6): 449-56.

[11] Digital Medical Association of Chinese Medical Association, Digital Intelligent Surgery Professional Committee of Chinese Research Hospital Association, Medical Imaging and Equipment Professional Committee of China Graphics Society, et al. Expert consensus on application of computer-assisted indocyanine green molecular fluorescence imaging technology in the diagnosis and surgical navigation of liver tumor [J]. Chin J Pract Surg, 2017, 37(5): 531-8.

[12] Yang J, Fang CH, Fan YF, et al. To assess the benefits of medical image three-dimensional visualization system assisted pancreaticoduodenctomy for patients with hepatic artery variance [J]. Int J Med Robot, 2014, 10(4): 410-17.

[13] Digital Medical Association of Chinese Medical Association, Digital Intelligent Surgery Professional Committee of Chinese Research Hospital Association. Expert consensus on precise diagnosis and treatment of complex liver tumors based on three-dimensional visualization technology[J]. Chin J Pract Surg, 2017, 37(1): 53-9.

[14] Huang L, Vore M. Multidrug resistance p-glycoprotein 2 is essential for the biliary excretion of indocyanine green[J]. Drug Metab Dispos, 2001, 29(5): 634-7.

[15] De Graaf W, Hausler S, Heger M, et al. Transporters involved in the hepatic uptake of (99m)Tc-mebrofenin and indocyanine green[J]. J Hepatol, 2011, 54(4): 738-45.

[16] Alander J T, Kaartinen I, Laakso A, et al. A review of indocyanine green fluorescent imaging in surgery[J]. Int J Biomed Imaging, 2012, 2012: 940585.

[17] Desmettre T, Devoisselle JM, Mordon S. Fluorescence properties and metabolic features of indocyanine green (ICG) as related to angiography[J]. Surv Ophthalmol, 2000, 45(1): 15-27.

[18] Takahashi H, Zaidi N, Berber E. An initial report on the intraoperative use of indocyanine green fluorescence imaging in the surgical management of liver tumors[J]. J Surg Oncol, 2016, 114(5): 625-9.

[19] Kaibori M, Ishizaki M, Matsui K, et al. Intraoperative indocyanine green fluorescent imaging for prevention of bile leakage after hepatic resection[J]. Surgery, 2011, 150(1): 91-8.

[20] Miyata A, Ishizawa T, Tani K, et al. Reappraisal of a dye-staining technique for anatomic hepatectomy by the concomitant use of indocyanine green fluorescence imaging[J]. J Am Coll Surg, 2015, 221(2): e27-36.

[21] Tomassini F, Scarinci A, Elsheik Y, et al. Indocyanine green near-infrared fluorescence in pure laparoscopic living donor hepatectomy: a reliable road map for intra-hepatic ducts [J]? Acta Chir Belg, 2015, 115(1): 2-7.

[22] Speich R, Saesseli B, Hoffmann U, et al. Anaphylactoid reactions after indocyanine-green administration[J]. Ann Intern Med, 1988, 109(4): 345-6.

[23] Zhu W, Fang CH, Fan YF, et al. Construction and clinical application of three-dimensional visualization platform in diagnosis and treatment of primary liver cancer [J]. Chin J Hepat Surg (Electronic Edition), 2015, 4(5): 268-73.

[24] Lim C, Vibert E, Azoulay D, et al. Indocyanine green fluorescence imaging in the surgical management of liver cancers: Current facts and future implications[J]. J Visc Surg, 2014, 151(2): 117-24.

[25] Dahiya D, Wu TJ, Lee CF, et al. Minor versus major hepatic resection for small hepatocellular carcinoma (HCC) in cirrhotic patients: a 20-year experience [J]. Surgery, 2010, 147(5): 676-85.

[26] Zhang Y, Shi R, Hou J, et al. Liver tumor boundaries identified intraoperatively using real-time indocyanine green fluorescence imaging[J]. J Cancer Res Clin Oncol, 2017, 143(1): 51-8.

[27] International Consensus Group for Hepatocellular Neoplasia. Pathologic diagnosis of early hepatocellular carcinoma: a report of the international consensus group for hepatocellular neoplasia[J]. Hepatology, 2010, 49(2): 658-64.

[28] Fomer A, LloVet JM, Bmix J. Hepatocellular carcinoma. Lancet, 2012, 379: 1245-55.

[29] Tanaka S, Hirohashi K, Tanaka H, et al. Incidence and management of bile leakage after hepatic resection for malignant hepatic tumors [J]. J Am Coll Surg, 2002, 195(4): 484-9.

[30] Nagano Y, Togo S, Tanaka K, et al. Risk factors and management of bile leakage after hepatic resection[J]. World J Surg, 2003, 27(6): 695-8.

[31] Linke R, Ulrich F, Bechstein WO, et al. The White-test helps to reduce biliary leakage in liver resection: a systematic review and meta-analysis[J]. Ann Hepatol, 2015, 14(2): 161-7.

[32] Guillaud A, Pery C, Campillo B, et al. Incidence and predictive factors of clinically relevant bile leakage in the modern era of liver resections[J]. HPB (Oxford), 2013, 15(3): 224-9.

[33] Mullock BM, Shaw LJ, Fitzharris B, et al. Sources of proteins in human bile[J]. Gut, 1985, 26(5): 500-9.

[34] Sakaguchi T, Suzuki A, Unno N, et al. Bile leak test by indocyanine green fluorescence images after hepatectomy[J]. Am J Surg, 2010, 200(1): e19-23.

[35] Tanaka M, Inoue Y, Mise Y, et al. Laparoscopic deroofing for polycystic liver disease using laparoscopic fusion indocyanine green fluorescence imaging[J]. Surg Endosc, 2016, 30(6): 2620-3.

[36] Shrikhande SV, Kleeff J, Reiser C, et al. Pancreatic resection for M1 pancreatic ductal adenocarcinoma[J]. Ann Surg Oncol, 2007, 14(1): 118-27.

[37] Seelig S K, Burkert B, Chromik AM, et al. Pancreatic resections for advanced M1-pancreatic carcinoma: the value of synchronous metastasectomy[J]. HPB Surg, 2010, 2010: 579672.

[38] Peloso A, Franchi E, Canepa MC, et al. Combined use of intraoperative ultrasound and indocyanine green fluorescence imaging to detect liver metastases from colorectal cancer[J]. HPB, 2013, 15(12): 928-34.

[39] Yokoyama N, Otani T, Hashidate H, et al. Real-time detection of hepatic micrometastases from pancreatic cancer by intraoperative fluorescence imaging[J]. Cancer, 2012, 118(11): 2813-9.

[40] Weissleder R. A clearer vision for in vivo imaging[J]. Nat Biotechnol, 2001, 19(4): 316-7.

[41] Howanitz PJ, Hoffman GG, Zarbo RJ. The accuracy of frozen-section diagnoses in 34 hospitals[J]. Arch Pathol Lab Med, 1990, 114(4): 355-9.

[42] Ishizawa T, Zuker NB, Kokudo N, et al. Positive and negative staining of hepatic segments by use of fluorescent imaging techniques during laparoscopic hepatectomy[J]. Arch Surg, 2012, 147(4): 393-4.

[43] Mizuno S, Isaji S. Indocyanine green (ICG) fluorescence imaging-guided cholangiography for donor hepatectomy in living donor liver transplantation[J]. Am J Transplant, 2010, 10(12): 2725-6.

[44] Kubota K, Kita J, Shimoda M, et al. Intraoperative assessment of reconstructed vessels in living-donor liver transplantation, using a novel fluorescence imaging technique[J]. J Hepatobiliary Pancreat Surg, 2006, 13(2): 100-4.

[45] Gotoh K, Yamada T, Ishikawa O, et al. A novel image-guided surgery of hepatocellular carcinoma by indocyanine green fluorescence imaging navigation[J]. J Surg Oncol, 2009, 100(1): 75-9.

[46] Liao WJ, Mao YL. Standardized management of liver cancer during perioperative period[J]. Chin J Pract Surg, 2014, 8: 783-5.

[47] Chen Q, Shu C, Laurence AD, et al. Effect of Huaier granule on recurrence after curative resection of HCC: a multicentre, randomised clinical trial[J]. Gut, 2018, 67(11): 2006-16.

2019

中华医学会数字医学分会；中国研究型医院学会数字智能化专业委员会；中国医师协会肝癌专业委员会；中国医师协会临床精准医学专业委员会；中国图学学会医学图像与设备专业委员会；中国生物物理学会分子影像学专业委员会

摘要：计算机辅助联合吲哚菁绿分子荧光影像技术可以从三维的形态解剖和细胞功能水平进行术前规划和术中侦测，从而导航肝癌解剖性、功能性、根治性的肝切除术，临床应用证明其有重要的诊疗价值，此项技术现已在全国得到了广泛推广和应用。为规范计算机辅助联合吲哚菁绿分子荧光影像技术在肝脏肿瘤精准诊疗中的应用，本指南在以下几个方面进行了研究：(1)三维可视化技术应用流程；(2)ICG分子荧光成像的机制及应用流程；(3)三维可视化和虚拟现实技术的临床应用；(4)ICG分子荧光影像技术的临床应用。ICG分子荧光成像技术能从分子、细胞水平层面实现肿瘤边界界定、肝段和肝叶切除切线的确定；微小病灶或转移灶的侦测；术中根据肝脏肿瘤的荧光信号特点，结合术中快速冰冻病理学检查，可初步判定肝脏占位性病变的分化程度；肝切除后对肝断面进行残留肿瘤病灶和胆漏的检测。计算机辅助联合ICG分子荧光影像技术在肝脏肿瘤诊断和手术导航中的应用，为肝脏肿瘤的外科治疗提供了一种新的数字智能化外科诊疗技术，该项技术亦将不断改进和完善，为肝脏肿瘤的精准诊疗展现出良好的应用前景。

关键词：吲哚菁绿；荧光影像；三维可视化；肝脏肿瘤；导航手术

作者简介：方驰华，E-mail: fangch_dr@126.com，南方医科大学珠江医院肝胆一科，广东省数字医学临床工程技术研究中心